

Received: 2018.08.23

Accepted: 2018.11.13

Published: 2018.12.12

Silencing the ACAT1 Gene in Human SH-SY5Y Neuroblastoma Cells Inhibits the Expression of Cyclo-Oxygenase 2 (COX2) and Reduces β -Amyloid-Induced Toxicity Due to Activation of Protein Kinase C (PKC) and ERK

Authors' Contribution:

Study Design A
Data Collection B
Statistical Analysis C
Data Interpretation D
Manuscript Preparation E
Literature Search F
Funds Collection G

ABCDEF 1,2 **Ying Chen***
ABCEF 2,3 **Lu Zhu***
B 2 **Lei Ji**
CD 2 **Ying Yang**
ACD 4 **Lu Lu**
ACDEG 2 **Xiaodong Wang**
ADEF 1 **Guomin Zhou**

1 Department of Anatomy, Histology and Embryology, School of Basic Medical Sciences, Fudan University, Shanghai, P.R. China
2 Department of Histology and Embryology, Medical College, Nantong University, Nantong, Jiangsu, P.R. China
3 Department of Human Anatomy, College of Basic Medicine, Xinjiang Medical University, Xinjiang, Urumqi, P.R. China
4 Department of Genetics, Genomics and Informatics, University of Tennessee Health Science Center, Memphis, TN, U.S.A.

* Ying Chen and Lu Zhu contributed equally to this work

Corresponding Author: Guomin Zhou, e-mail: gmzhou@shmu.edu.cn

Source of support: This work was supported by the grants from the National Natural Science Foundation of China (Grant No. 31571238, 31570983, and 81200828) and the Natural Science Foundation of the Jiangsu Higher Education Institutions of China (Grant No. 16KJB310011)

Background: Acyl-coenzymeA: cholesterol acyltransferase (ACAT) 1, a key enzyme converting excess free cholesterol to cholesterol esters, has been demonstrated to be associated with the pathogenesis of Alzheimer disease (AD). However, the mechanism underlying the protective role of ACAT1 blockage in AD progression remains elusive.


Material/Methods: Human neuroblastoma SH-SY5Y cells were treated for 24 h with increasing concentrations of aggregated $A\beta_{25-35}$ (5, 15, 25, and 45 μ mol) with or without the ACAT1 siRNA pretreatment. Cell viability analysis was measured by CCK-8 assay. The genome-wide correlation between ACAT1 and all other probe sets was measured by the Pearson correlation coefficient (*r*). Western blotting was used to detect the ACAT1 protein expression in the hippocampus of APP/PSN transgenic AD mice. The mRNA level for each target was analyzed by qPCR. Western blotting was used to detect the ACAT1, cyclo-oxygenase-2 (Cox2), Calcium voltage-gated channel subunits (CACNAs), and ERK/PKC proteins in SH-SY5Y cells with or without the ACAT1 siRNA pretreatment in the presence of $A\beta_{25-35}$.

Results: The expression of ACAT1 was significantly increased in the hippocampus of APP/PSN mice, and also showed an increasing trend when SH-SY5Y cells were exposed to $A\beta_{25-35}$. Silencing ACAT1 significantly attenuated $A\beta$ -induced cytotoxicity and cell apoptosis in SH-SY5Y cells. The genome-wide correlation analysis showed that *Ptgs2* had the most significant correlation with *Acat1* in the hippocampus of BXD RI mice. We further determined the regulatory effect of ACAT1 on COX2 expression by silencing or over-expressing ACAT1 in SH-SY5Y cells and found that silencing ACAT1 played a protective role in AD progression by regulating CACNAs and PKC/ERK signaling cascades.

Conclusions: Silencing ACAT1 attenuates $A\beta_{25-35}$ -induced cytotoxicity and cell apoptosis in SH-SY5Y cells, which may due to the synergistic effect of ACAT1 and COX2 through PKC/ERK pathways.

MeSH Keywords: **Acyl-coenzymeA: Cholesterol Acyltransferase • Alzheimer Disease • Cyclooxygenase 2**

Full-text PDF: <https://www.medscimonit.com/abstract/index/idArt/912862>

 3539

 2

 5

 40



Background

Alzheimer disease (AD) is the most common form of dementia. AD is characterized by senile plaques (SP) created by progressive accumulation of amyloid β -peptide ($A\beta$) and neurofibrillary tangles (NFT) composed of hyper-phosphorylated tau in brain regions. Growing evidence suggests that cellular cholesterol homeostasis is closely associated with AD pathogenesis, especially in amyloidogenesis [1,2]. In the brain, cholesterol is mainly derived from *de novo* synthesis via the hydroxymethyl glutaryl-CoA (HMG-CoA) reductase pathway, and is present mainly in its unesterified form in myelin sheaths and the cellular membranes of glial cells and neurons [3]. Within the cells, cholesterol is found in two forms: free cholesterol (FC) and cholesterol esters (CE). Acyl-coenzymeA: cholesterol acyltransferase (ACAT, also known as sterol O-acyltransferase, abbreviated as SOAT) catalyzes excess FC in cells into CE and mediates cellular cholesterol homeostasis [2]. There are two ACAT isoforms in mammals – ACAT1 and ACAT2 [4] – with different tissue expression patterns. ACAT1 is a resident enzyme at the endoplasmic reticulum and is ubiquitously expressed in all tissues, whereas ACAT2 is mainly expressed in the intestines and hepatocytes [5].

Although the molecular basis of the relationship between cholesterol homeostasis and AD pathogenesis is unclear, much attention also has been paid to seeking novel therapeutic targets such as statins (HMG-CoA reductase inhibitor) [6,7] and ACAT1 inhibitors [8]. Previous animal experiments showed that $A\beta$ generation and deposition were reduced upon pharmacological inhibition of ACAT1 or by knocking out the ACAT1 gene [9,10]. Recent studies by Shibuya et al. demonstrated that ACAT1 inhibition induced an inhibitory effect against AD in neurons and microglia by stimulating autophagy. Surprisingly, the enhancing effect of ACAT1 blockage did not alter mTOR signaling or endoplasmic reticulum stress response [11,12]. The exact mechanism needs to be further explored.

ACAT1 is a key regulator in cellular cholesterol homeostasis and is associated with AD pathogenesis. However, the mechanism underlying the protective role of ACAT1 blockage in AD progression remains elusive. Previously, we have used the genetic genomics approach to dissect the genetic regulatory network for complex diseases, such as stress responses [13] and Parkinson disease [14]. The aim of the present study was to investigate the role of ACAT1 in APP/PSN double-transgenic AD mice and in human neuroblastoma SH-SY5Y cells. Genome-wide analysis was carried out in BXD RI mice to determine the regulatory gene network of *Acat1* and to identify transcripts that co-vary with *Acat1*, which may function in the same biological network and contribute to the pathogenesis of AD. We were particularly interested in the most significant correlation between *Acat1* and prostaglandin-endoperoxide synthase 2 (*Ptgs2*). *PTGS2* encodes cyclo-oxygenase-2 (COX-2),

a key enzyme in prostaglandin biosynthesis, and acts as a pro-inflammatory mediator implicated in the pathogenesis of neurodegenerative diseases [15,16]. In addition, we attempted to validate the interaction between ACAT1 and COX2 and evaluate mechanisms underlying the protective effect of ACAT1 silencing in $A\beta$ -induced SH-SY5Y cells.

Material and Methods

Animals

All animal experiments were conducted in compliance with the Institutional Animal Care guidelines and ethics approval was granted by the Administration Committee of Jiangsu Province, China. Transgenic B6/JNju-Tg (APP^{swe}, PSEN1^{dE9}) (abbreviated as APP/PSN) mice were obtained from the Model Animal Research Center of Nanjing University, and age- and sex-matched (10-month-old males) wild-type C57BL/6J mice were used as controls.

Cell culture, $A\beta$ treatment, and cell viability analysis

The human neuroblastoma cell line SH-SY5Y is commonly used in studies of neurotoxicity, oxidative stress, and neurodegenerative diseases. In the present study, SH-SY5Y cells (Shanghai Institute of Materia Medica, Chinese Academy of Sciences) were routinely grown in Dulbecco's modified Eagle's medium (Corning Life Sciences), supplemented with 10% fetal bovine serum. $A\beta_{25-35}$ was purchased from Sigma-Aldrich. As previously described [17], $A\beta_{25-35}$ was dissolved in sterilized double-distilled water at a concentration of 1 mM/ml and incubated at 37°C for 7 days to form an aggregated form. Cell viability analysis was performed using Cell Counting Kit-8 (CCK-8) assay (Beyotime). Briefly, cells were pre-incubated in 96-well plates at a density of 5×10^4 cells for 20 h, incubated with different concentrations of aggregated $A\beta_{25-35}$ (5, 15, 25, and 45 μ mol) for 24 h, and then incubated again with CCK-8 solution according to the manufacturer's instructions.

Plasmid and siRNA transfection

Cells grown to ~70% confluence were transfected with 50–100 nM siRNAs (Biomic) to target ACAT1 or *PTGS2* in SH-SY5Y cells (Table 1), and a scrambled siRNA was used as control. The ACAT1 plasmid was purchased from Genechem, and empty vector was used as the control (referred to here as vector). Transfection of siRNA and plasmids was performed using Lipofectamine 2000 reagent (Invitrogen) according to the manufacturer's instructions.

RNA extraction and qPCR

Total RNA was extracted by using the RNeasy Mini kit (QIAGEN) according to the manufacturer's instructions. cDNA was prepared

Table 1. Primers and siRNAs used in this study.

Primers/siRNAs	Sequence (5'-3')
β-actin_F	CGTTGACATCCGTAAGACC
β-actin_R	TAGAGCCACCAATCCACAC
ACAT1_F	CATCCTATTCGTCCTCAG
ACAT1_R	GGGTAGTTGTCTCGGTAA
COX2_F	AACAGGGAGGTGCTGTACG
COX2_R	TGTAGCTCCTTGGTGAAGCA
hs-ACAT1-si-1	GCUCUCUCUUGAUGAACU
hs-ACAT1-si-2	CCCACUCAUUUGUCAGAGA
hs-ACAT1-si-3	CUCUUCAUGUUCUUUGGAA
hs-PTGS2-si-1	CUUACCCACUUC AAGGGAU
hs-PTGS2-si-2	CCUCAAUUCAGUCUCUCAU
hs-PTGS2-si-3	GAAUCAUUCACCAGGCAAA

by reversely transcribing total RNA (2 μg) using SuperScript III reverse transcriptase (Thermo Scientific). The mRNA level for each target was analyzed by qPCR using iTaq Universal SYBR Green Supermix (Bio-Rad) with Bio-Rad CFX manager 3.1. Primers used in this study are listed in Table 1. Relative quantification was determined using the CT method. The mRNA expression values were normalized with β-actin mRNA level.

Protein extraction and Western blotting

The tissue and cell samples were washed with ice-cold PBS and incubated for 30 min on the ice in lysis buffer. The supernatant was retained after centrifugation. Protein concentration was determined using the BCA protein assay kit (Pierce). For Western blot analysis, 100 μg total protein from each sample was separated on SDS-PAGE gel and transferred onto PVDF membranes. The membranes were blocked with 5% milk blocking buffer and incubated with the designed primary antibodies overnight at 4°C. The primary antibodies are listed in Table 2. After 3 washes with TBS, the membranes were incubated with HRP-conjugated secondary antibody at 37°C for 2 h. Bound secondary antibodies were visualized using an enhanced chemiluminescence (ECL) kit (Bio-Rad) with ChemDoc XRS and Quantity One software (Bio-Rad).

Gene network data sets

All data sets used in this study can be publically accessed from www.genenetwork.org. The primary data set used was “Hippocampus Consortium M430v2.0 (Jun06) RMA”, which includes steady-state transcript abundance measurements collected from the hippocampus of 67 BXD RI strains, 2 reciprocal F1 hybrids, and the B6 and D2 parental strains, using the

Table 2. Primary antibodies used in the present study.

Antibody	Dilution	Manufacturer
Rabbit anti-ACAT1	1: 500	Abcam, Cambridge, UK
Goat anti-COX-2	1: 500	Abcam
Mouse anti-PKC	1: 1000	Abcam
Mouse anti-ERK1/2	1: 1000	Abcam
Rabbit anti-Caspase3	1: 1000	Abcam
Rabbit anti-Cacna1b	1: 1000	Alomone Labs, Jerusalem, Israel
Rabbit anti- Cacna2d1	1: 1000	CMCTAG, San Diego, USA
Mouse anti-β-actin	1: 5000	

Affymetrix Mouse Genome 430 2.0 array. Detailed information for data sets can be found in the “Info” page at www.genenetwork.org.

Correlation analysis and gene network construction

The correlation between *Acat1* (probe set 1417696_at) and all other probe sets in the Hippocampus Consortium M430v2.0 data set was analyzed by Pearson product-moment correlation analysis. Significant correlations (*P* Value of correlation <0.0001) with the expression level greater than 8 units were selected to construct the gene co-regulatory network for *Acat1* by using Spring Model Layout Network Graphs in GeneNetwork (www.genenetwork.org) [18].

Statistical analysis

All data are expressed as means ±SEM. All statistical analyses were performed using Prism software (GraphPad). A two-tailed *t* test was used when 2 values were compared. For multiple comparisons, a one-way ANOVA with a Turkey’s post test was used. *P* values less than 0.05 were considered to be statistically significant.

Results

Elevated expression of ACAT1 in Alzheimer Disease mouse and cell models

To explore the possible role of ACAT1 in the pathogenesis of AD, the expression of ACAT1 was detected in APP/PSN and age-matched wild-type (WT) C57BL/6J mice. Compared to the WT group, the expression level of ACAT1 significantly elevated in hippocampus of APP/PSN mice (Figure 1A). ACAT1

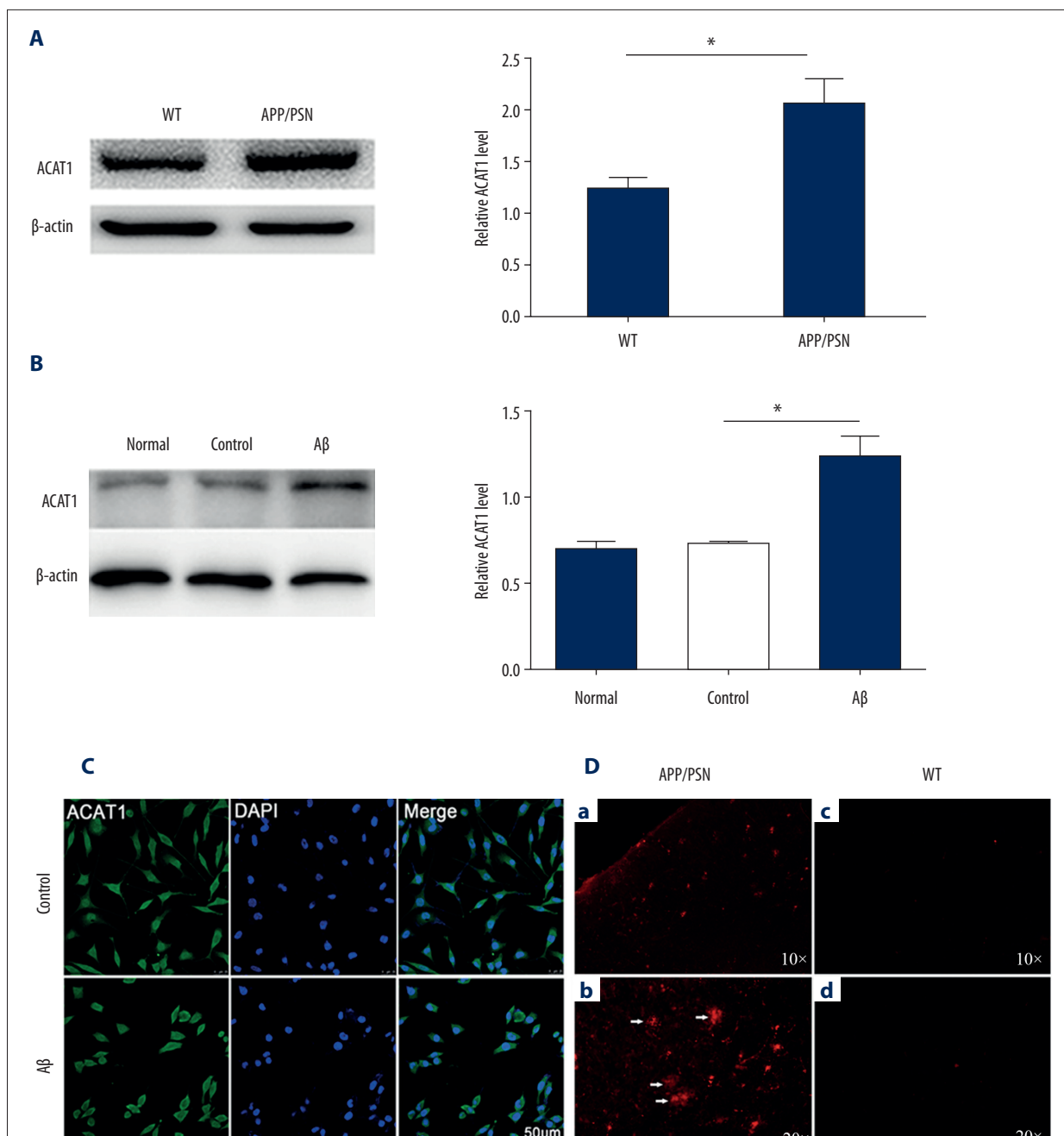


Figure 1. Expression of ACAT1 in Alzheimer Disease mouse and cell models. **(A)** The expressions of ACAT1 in hippocampus of APP/PSN mice and wild-type (WT) group were detected using Western blotting (* $P < 0.05$, $N = 3$). **(B)** Representative image of immunoblots for ACAT1 (***) $P < 0.001$, versus control group) in SH-SY5Y cells under normal condition (DMEM with FBS, Normal), control condition (DMEM without FBS, Control), and $A\beta_{25-35}$ treatment ($A\beta$). **(C)** Anti-ACAT1 immunofluorescence staining in SH-SY5Y cells showed cellular morphological changes after $A\beta_{25-35}$ treatment. **(D)** The immunoreactivity of $A\beta$ was determined by immunohistochemistry with an anti- $A\beta$ antibody in Cortex of APP/PSN mice **(a, b)** and wild-type (WT) group **(c, d)**. The white arrows indicate $A\beta$ plaques. These results are representative of 3 independent experiments with each condition triplicated.

expression was also evaluated in SH-SY5Y cells exposed to $A\beta_{25-35}$. Western blot analysis showed a significant rise in ACAT1 expression after treatment with $A\beta_{25-35}$ (Figure 1B). Anti-ACAT1

immunofluorescence staining in SH-SY5Y cells showed cellular morphological changes after $A\beta_{25-35}$ treatment, of which the cell's processes became shorter or disappeared (Figure 1C).

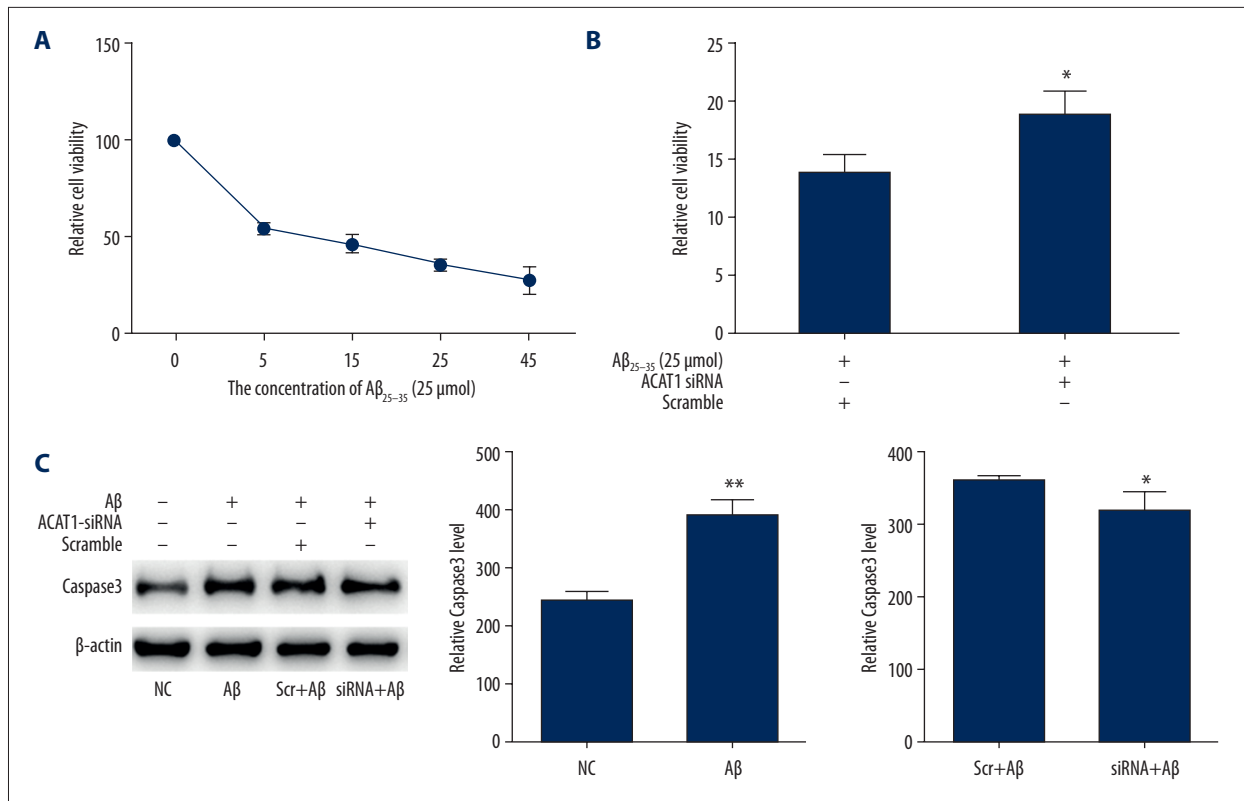


Figure 2. Silencing ACAT1 inhibited Aβ₂₅₋₃₅-induced cytotoxicity and cell apoptosis in SH-SY5Y neuroblastoma cells. (A) SH-SY5Y cells were treated with Aβ₂₅₋₃₅ (5, 15, 25, and 45 μmol) for 24 h and cell viability was analyzed by CCK-8 assay. (B) Silencing ACAT1 significantly inhibited Aβ₂₅₋₃₅ induced cytotoxicity. (C) Silencing ACAT1 or not before Aβ₂₅₋₃₅ treatment, total cell lysates of SH-SY5Y cells were harvested. Expression of caspase-3 and β-actin was determined by Western blotting. Results were presented as mean ±SD of 3 independent experiments. (** *P*<0.01 and * *P*<0.05).

Silencing ACAT1 attenuates Aβ₂₅₋₃₅-induced cytotoxicity and cell apoptosis in SH-SY5Y neuroblastoma cells

CCK-8 assay showed that Aβ₂₅₋₃₅ significantly decreased cell viability in a concentration-dependent manner (Figure 2A). Cell viability was reduced to 32.78% and 26.78% after exposure to 25 and 45 μmol Aβ₂₅₋₃₅ for 24 h, respectively. In the subsequent experiments, 25 μmol/L Aβ₂₅₋₃₅ was chosen as the optimal concentration to induce neurotoxicity. To evaluate the potential role of ACAT1 in Aβ₂₅₋₃₅-induced SH-SY5Y cells, we inhibited the ACAT1 expression before Aβ₂₅₋₃₅ treatment. The result showed that ACAT1_siRNA-2 had the strongest interfering effect by downregulating the ACAT1 mRNA level by 27.88%, and thus was used for subsequent RNAi experiments. CCK-8 assay showed that cell death was reduced, and cell viability was 19% in the pre-silencing ACAT1 treatment group vs. 14% in the scramble group (*P*<0.05) (Figure 2B), indicating that ACAT1 pre-silencing played a protective role against Aβ-induced SH-SY5Y cell death.

The protein level of caspase-3 (32 kD) was increased by 1.5-fold after Aβ₂₅₋₃₅ (25 μmol/L) treatment (*P*<0.05) (Figure 2C).

However, in the ACAT1_siRNA pretreated group (ACAT1_siRNA+Aβ₂₅₋₃₅ group), the relative expression level of caspase-3 was significantly decreased (*P*<0.05) (Figure 2C) compared with the control group (Scramble siRNA+Aβ₂₅₋₃₅ group), suggesting that ACAT1 pre-silencing counteracts Aβ-induced apoptosis by inhibiting caspase3 activation.

Genes significantly correlated with *Acat1* expression were collected from the BXD RI mouse hippocampus for correlation analysis

To identify potential mechanisms underlying the protective role of *Acat1* silencing in AD progression, we queried the Hippocampus Consortium M430v2 (Jun 06) RMA data set to identify transcripts that co-vary with *Acat1*. Expression of *Acat1* on the Affymetrix MOE430V2 array was interrogated by 5 probe sets. The expression level of *Acat1* measured by probe set 1417696_at varied 1.5-fold across strains, with a mean expression of 8.48, and exhibited a trend of continuous change (Figure 3A). Pearson correlation analysis between *Acat1* (probe set 1417696_at) and whole mouse genome transcripts in the hippocampus of the BXD RI mice revealed that 375 probe sets

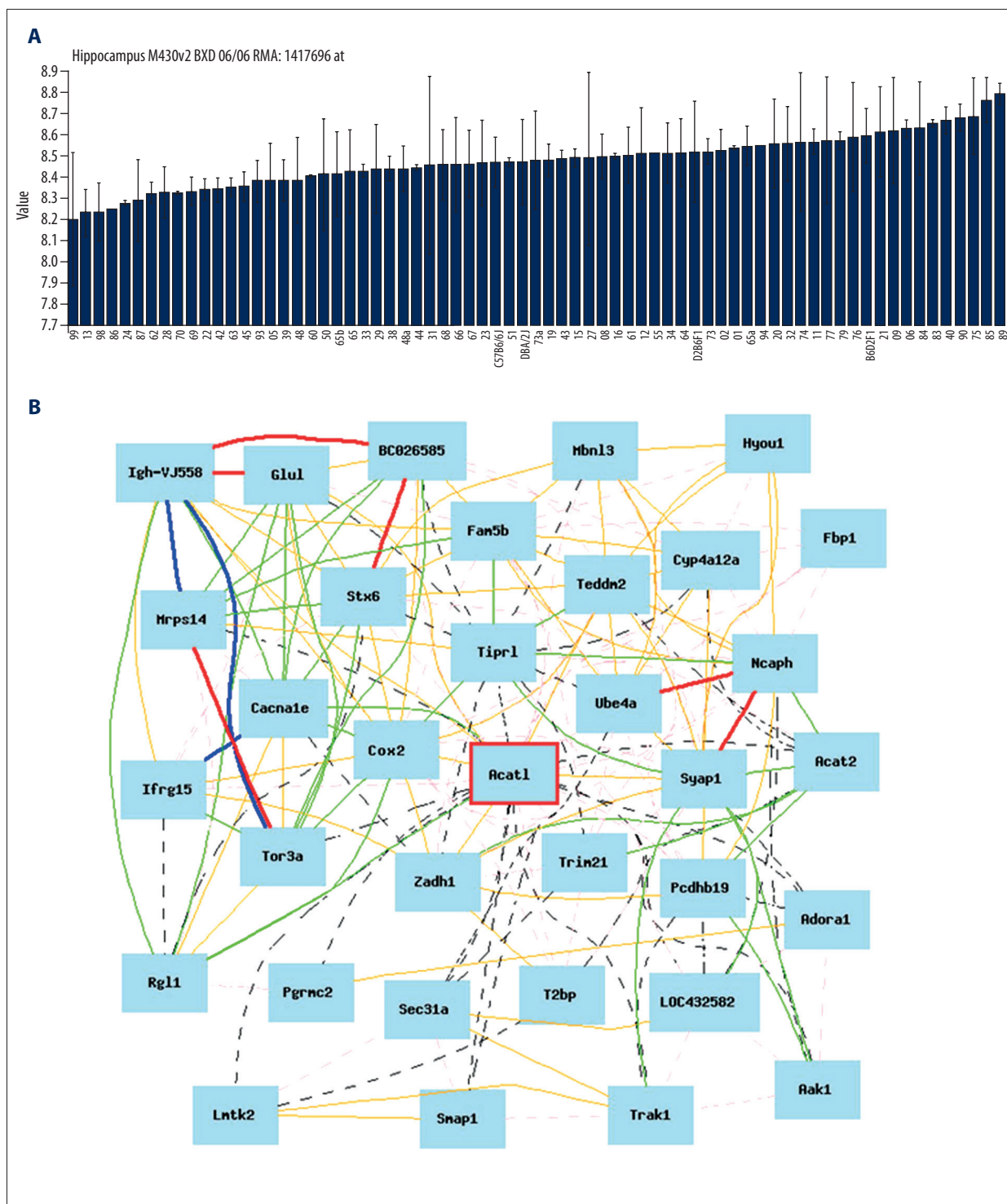


Figure 3. Expression variation and Gene network analysis of *Acat1* in hippocampus of BXD RI mice. **(A)** The expression level of *Acat1* measured by probe set 1417697_at among BXD RI strains varies 1.5-fold across strains with an average expression of 8.48. Values denote normalized relative expression levels. Strain names are indicated along the x axis. **(B)** Thirty-four genes were highly correlated with *Acat1* ($P < 0.0001$), with a mean expression level > 8 units in the hippocampal tissue. The degree of correlation between genes was described by the Pearson correlation coefficient. The bold/thin/dashed line reflects the coefficient of 1.0–0.7, 0.7–0.5, and 0.5–0.0, respectively. The red/orange/pink color indicates a positive correlation, and the blue/green/dark color indicates a negative correlation.

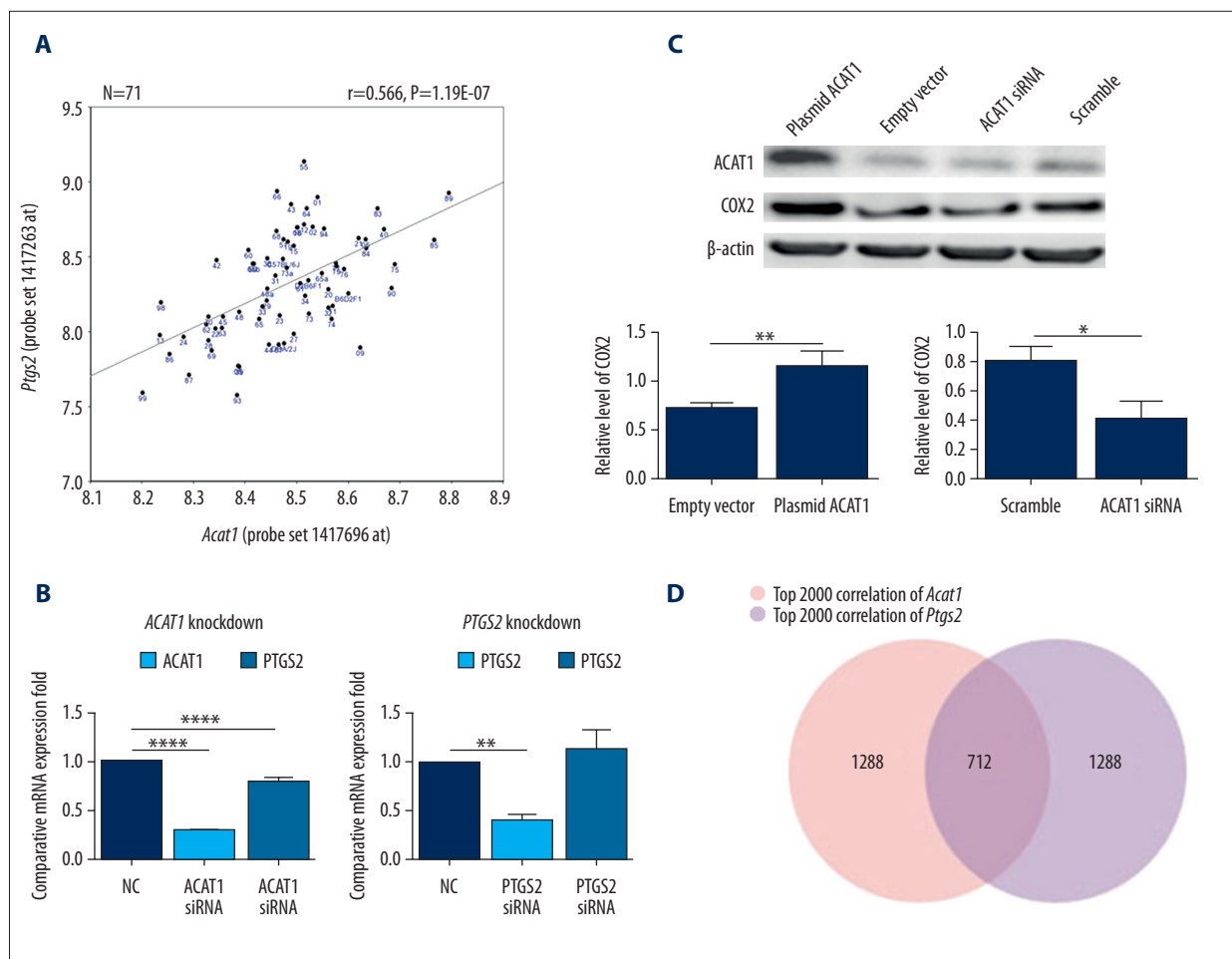
were significantly correlated with *Acat1* (P Value of Sample correlation <0.001). To graphically evaluate the strength of the Pearson correlation coefficients, we further selected 34 genes with expression levels greater than 8 units and significantly correlated with *Acat1* ($P<0.0001$) to generate a co-expression network (Figure 3B). The most significant correlation was *Ptgs2* (probe set 1417263_at) ($r=0.57$, $P=2.09E-07$). Cyclooxygenase-2 (COX-2), the rate-limiting enzyme responsible for prostaglandin production, has been shown to play a key role in the regulation of inflammation, and has received attention as a therapeutic target for AD [15]. Matrix analysis showed a near-linear dependency between the expression variations of these 2 genes in different strains of RI BXD mice ($R=0.615$) (Figure 4A). These findings indicate a complex synergistic action between *Acat1* and *Ptgs2*. Consequently, we focused on the relationship between *Acat1* and *Cox2* in further experiments.

To confirm the interaction between *ACAT1* and *PTGS2*, qPCR was performed to detect the expression levels in SH-SY5Y cells after *ACAT1*_siRNA and *PTGS2*_siRNA treatment, respectively. QPCR was used to detect the efficiency of different sequences of siRNA, and *ACAT1*_siRNA-2 and *PTGS2*_siRNA-2 were selected

for the following experiments. Knockdown of *ACAT1* mRNA reached 28.88% compared with the scrambled siRNA control group, while *PTGS2* decreased to 79.54% (Figure 4B, left). However, in the condition of *PTGS2* inhibition (knock down to 40.74%), the gene expression of *ACAT1* did not change significantly (Figure 4B, right). Western Blot analysis revealed that COX2 was decreased significantly after *ACAT1*-siRNA treatment ($P<0.05$). To further validate the regulatory effect, SH-SY5Y cells were transfected with plasmid-over-expressed *ACAT1*. Western blot analysis revealed that the relative expression of COX2 was increased by 1.61-fold after *ACAT1* plasmid transfection (Figure 4C). The above results suggest that COX2 expression is regulated by *ACAT1* in SH-SY5Y neuroblastoma cells

Potential mechanisms responsible for the protective effect of ACAT1 silencing in Aβ-induced SH-SY5Y cells

The top 2000 correlated genes in the Hippocampus Consortium M430v2 (Jun 06) RMA dataset for both *Acat1* and *Ptgs2* were identified by Pearson product-moment correlation analysis, and the common co-variations in both genes were further collected through VENN analysis. We found that 712 genes with varied



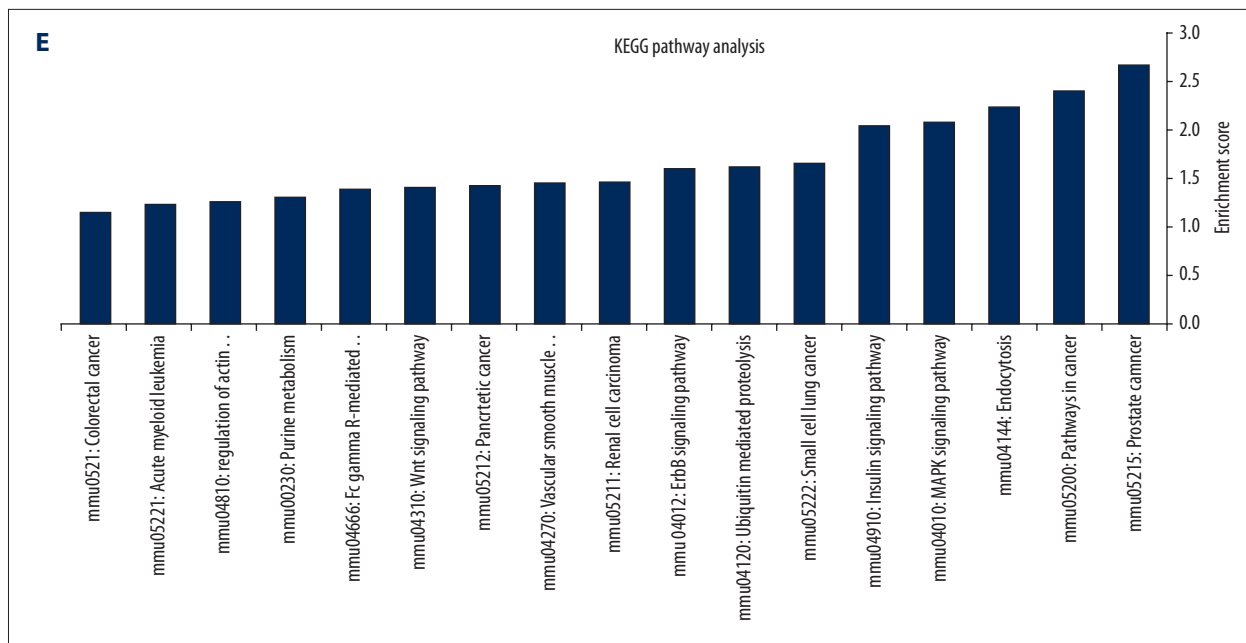


Figure 4. Correlation analysis and the expression regulation validation between *Acat1* and *Ptgs2*. (A) Correlation Matrix analysis for *Acat1* and *Ptgs2* expression in BXD RI mouse hippocampus (n=71). X axis and Y axis denoted *Acat1* and *Ptgs2* expression, respectively. Digitally labeled dots denote the 69 strains of BXD RI mice and parental strains (C57BL/6J) and DBA/2J). $P=1.19E-07$. (B) QPCR was performed to detect the contribution of ACAT1_siRNA to *Ptgs2* expression variation (B, left) and PTGS2_siRNA treatment to ACAT1 expression variation (B, right) in human SH-SY5Y cells. (C) Western Blot analysis was performed to detect COX2 protein changes after silencing or overexpressing ACAT1. (***) $P<0.001$, (**) $P<0.01$ and (*) $P<0.05$. (D) The top 2000 correlated genes for both *Acat1* and *Ptgs2* in BXD RI mouse hippocampus were collected, and 712 genes were collected as the common co-variations with both genes through VENN analysis. Pink and purple cycles denote numbers of highly correlated genes with *Acat1* or *Ptgs2*, respectively. (E) KEGG pathway analysis revealed 17 significant enrichment pathways; X-axis and Y-axis denotes the enriched pathway and enriched index $-\log(P \text{ value})$, respectively.

expression were highly correlated with both genes, meaning that these genes may be involved in *Acat1* and *Ptgs2* interactions (Figure 4F). KEGG pathway analysis revealed several significant enrichment pathways, including endocytosis (mmu04144), and MAPK signaling pathway (mmu04010) (Figure 4E). We were particularly interested in the MAPK signaling pathway, which is known to be involved in the transcriptional regulation of several genes encoding for proinflammatory cytokines, and their altered phosphorylation states may lead to the development of inflammatory response in AD [19,20]. Calcium voltage-gated channel subunit alpha 1 B (CACNA1b) and calcium voltage-gated channel auxiliary subunit alpha 2 delta 1 (CACNA2d1), which contributed to the Voltage-Gated Calcium Channel Subunits category, were also enriched in the MAPK pathway. Western blot results showed that the relative expression of total PKC and the ratio of phospho-ERK (p-ERK)/ERK were decreased by 87.87% ($P<0.01$) and 26.3% ($P<0.05$), respectively, after $A\beta_{25-35}$ treatment as compared with the control group, suggesting that PKC and ERK are involved in $A\beta_{25-35}$ -induced cytotoxicity in SH-SY5Y cells. Meanwhile, the relative expression of CACNA1b and CACNA2d1 was increased by 1.63- and 1.81-fold, respectively, after $A\beta_{25-35}$ treatment (Figure 5A).

Effects of knockdown ACAT1 on PKC and ERK phosphorylation and CACNAs in $A\beta$ -induced SH-SY5Y cells

To further explore the effect of knock down of ACAT1 on the MAPK family, the amount of PKC and ERK phosphorylation and CACNAs was assessed by Western blot. The result showed that the relative expression of total PKC and the ratio of p-ERK/ERK were increased by 1.51- and 1.45-fold, respectively, after knockdown of ACAT1 in $A\beta$ -induced SH-SY5Y cells as compared with the control group ($P<0.05$) (Figure 5B). Knockdown of ACAT1 attenuated the reduction of p-ERK and PKC in $A\beta$ -induced SH-SY5Y cells. The relative expression of CACNA1b and CACNA2d1 was decreased by 72% ($P<0.01$) and 52.53% ($P<0.05$), respectively, after knockdown of ACAT1 in $A\beta$ -induced SH-SY5Y cells (Figure 5B). These results indicate that PKC and ERK signaling pathways might be involved in knockdown of ACAT1-mediated COX2 inhibition and neuroprotection in the AD cell model.

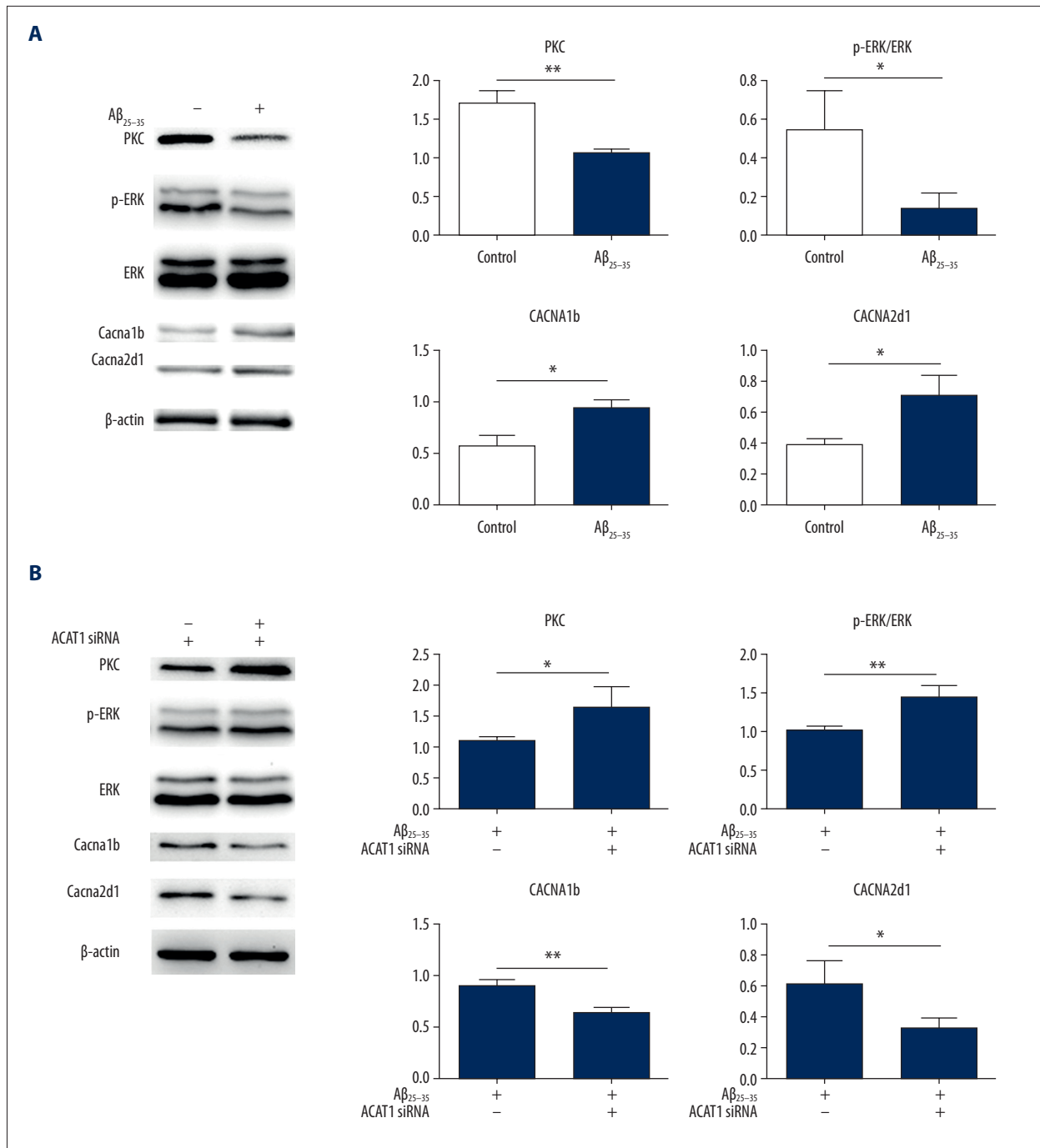


Figure 5. Effects of knockdown ACAT1 on CACNAs, PKC, and ERK phosphorylation and in Aβ-induced SH-SY5Y cells. **(A)** Western blot results showed that the relative expression of CACNA1b and CACNA2d1 was increased significantly, while the total PKC and the ratio of phospho-ERK (p-ERK)/ERK were decreased significantly after Aβ₂₅₋₃₅ treatment. **(B)** Knockdown of ACAT1 rescued the reduction of PKC and phosphorylation level of ERK, and also retarded the upregulation of CACNA1b and CACNA2d1 induced by Aβ. (** $P < 0.01$ and * $P < 0.05$).

Discussion

ACAT1 inhibitors have recently emerged as promising drug candidates. Previously, most efforts have been focused on targeting ACAT1 to treat atherosclerosis [21,22]. Recently, the potential effect of ACAT1 inhibitors in the treatment of AD [8] and tumors [23] has also aroused much attention. Yang et al. reported that cholesterol esterification by inhibiting ACAT1 could enhance the anti-tumor activity of CD8⁺ T cells [23]. *In vivo* experiments demonstrated that ACAT1 inhibition could increase A β clearance and ameliorate cognitive deficits in transgenic mice [9]. Shibuya et al. reported that ACAT1 inhibition could affect the level of autophagy in neurons [12] and microglial cells [11], which could further affect A β clearance. However, this autophagy was not associated with the mTOR pathway [11,12]. The exact mechanism needs to be further explored. To obtain a comprehensive understanding of the possible molecular role of ACAT1 inhibition in the prevention and treatment of AD, we established an *Acat1* gene regulatory network by using genome-wide association analysis in BXD RI mice.

Interestingly, *Ptgs2* and *Acat1* showed a very high correlation in the gene regulatory network established in our study. To the best of our knowledge, such a high correlation has not been reported in the literature before. PTGS2-encoded COX-2 is an important neuroinflammatory factor and is extensively involved in neuronal damage, inflammatory response, and neurodegenerative diseases [10,15]. An Alzheimer Disease Anti-inflammatory Prevention Trial (ADAPT) was initiated to test whether naproxen (a nonselective COX inhibitor) or celecoxib (a selective COX-2 inhibitor) could delay the onset of dementia in cognitively intact older adults with a family history of AD. However, the results showed both naproxen and celecoxib were unable to prevent the deterioration of cognitive function, suggesting that COX-2 is not suitable for use as the target for the prevention of AD [24]. Our study first demonstrated that SOAT1-encoding ACAT1 and PTGS2-encoding COX-2 had a very high correlation; ACAT1 knockdown in SH-SY5Y cells reduced the expression of COX2 significantly and ACAT1 over-expression upregulated the expression of COX2, while COX2 knockout did not have a significant effect on the expression of ACAT1 (Figure 4). These findings suggest that ACAT1 may be an upstream regulatory site of COX2. We postulate that the increased expression of COX2 upon A β stimulation in the present study may reflect a change in the overall environment and therefore should not be selected as the target of AD prevention, although this needs to be verified by more *in vivo* studies. Although COX-2 inhibitors alone cannot prevent AD, their role in the occurrence of AD should not be ignored. COX2 expression in the brain of AD patients was found to be upregulated. In addition, COX2 mediated neuroinflammation, neurodegeneration, and cognitive impairment in a rat model of AD [15]. COX2 may work together with

other AD-related factors such as ACAT1 to participate in the initiation of AD. This may be the reason why COX-2 inhibitors alone do not work effectively against AD. Synergistic genes of COX2 such as ACAT1 could be considered as the action target in future research on the prevention and treatment of AD. However, it is worth noting that COX1, another member of the COX family, has also been shown to play an important role in AD pathogenesis [25–29]. In the AD brain, clusters of COX-1 expressing microglia around amyloid plaques were identified in certain cortical layers [25]. Genetic deletion of COX-1 significantly attenuates the oxidative stress and neuronal damage in response to A β 1–42 [26]. The COX-1-selective inhibitor SC-560 improved spatial learning and memory, and reduced amyloid deposits and tau hyperphosphorylation [29]. In future work, we will further focus on whether COX1 participates in the synergistic effect of ACAT1 and COX2. It was found in this study that knockdown of ACAT1 exerted a protective effect against A β _{25–35} induced cytotoxicity in SH-SY5Y cells by inhibiting cell apoptosis and elevation of COX2 expression. In addition, we conducted a genetic correlation analysis on *Acat1* and *Cox2* and retrieved their common highly related genes, and found that this part of genes was enriched to 17 pathways, of which CACNA1b and CACNA2d1 were enriched to the MAPK pathway. The expression of CACNA1b and CACNA2d1 was elevated in A β -induced SH-SY5Y cells, and inhibition of ACAT1 decreased the expression of CACNA1b and CACNA 2d1, which was accompanied with decreased level of COX-2 and the increased level of p-ERK/ERK and PKC. These changes to some extent protected the A β _{25–35}-induced AD cell model. It was reported that the level of A β _{25–35}-induced PKC was decreased in PC12 cells, and activation of PKC reduced cell apoptosis [30]. The results of our study also confirmed that the level of PKC in SH-SY5Y cells was decreased 24 h after A β induction. However, PKC was increased after addition of A β _{25–35} to SH-SY5Y cells with previous knockout of ACAT1, suggesting that ACAT1 knockout could increase the level of PKC, which may prevent cell apoptosis. It was found in our study that the level p-ERK/ERK was decreased 24 h after addition of A β _{25–35} to SH-SY5Y cells. Some other studies used A β _{25–35} to induce PC12 cells [31], primary cortical neurons [32], and hippocampal neurons [33], and found that the level of ERK was decreased upon A β stimulation, resulting in cell death. Prostaglandin E (PGE)₂, the chief prostanoid resulting from COX-2 activity, binds to 4 G-protein-coupled PGE receptor, EP1-4, having differential signaling abilities [34,35]. It has been demonstrated that stimulation of EP4 receptors leads to phosphorylation of ERKs through a PI3K-dependent mechanism [34], and the activation of ERK is necessary to support EP4-mediated CT26 cell proliferation [36]. Taking these results together, we indicated that the increased level of p-ERK/ERK after ACAT1 inhibition was due to the synergistic effect of ACAT1 and COX2.

It is noteworthy that some studies demonstrated that statins protect cells against apoptosis by increasing the level of p-ERK and play a role in increasing the cognitive level and attenuating the progression of AD [7,37]. As statins can reduce the synthesis of cholesterol, they have been widely used in the treatment of atherosclerosis and other cardiovascular diseases [22]. Studies in recent years demonstrated that statins decrease the level of A β in animal models. Some retrospective case-control studies suggested that statins reduced the risk of AD, but clinical trials and prospective cohort studies have produced inconsistent and mixed results [38,39]. A more recent study suggested that statins reduce the risk of AD, pointing out a correlation between the use of statins and the decreased risk of AD, but this decreased risk depends on sex, race/ethnicity, and the type of statins used [40]. However, there are controversies over the preventive effect of high-dose statins on AD, knowing that the statins can inhibit HMG-CoA reductase and limit the early steps of cholesterol synthesis, thus reducing the formation of many intermediate products such as anti-oxidants, which may aggravate the pathological change of AD.

References:

1. Chang TY, Yamauchi Y, Hasan M et al: Cellular cholesterol homeostasis in Alzheimer's disease. *J Lipid Res*, 2017; 58: 2239–54
2. Di Paolo G, Kim TW: Linking lipids to Alzheimer's disease: Cholesterol and beyond. *Nat Rev Neurosci*, 2011; 12: 284–96
3. Zhang J, Liu Q: Cholesterol metabolism and homeostasis in the brain. *Protein Cell*, 2015; 6: 254–64
4. Cases S, Novak S, Zheng YW et al: ACAT-2, a second mammalian acyl-CoA: Cholesterol acyltransferase. Its cloning, expression, and characterization. *J Biol Chem*, 1998; 273: 26755–64
5. Chang TY, Chang CC, Lin S et al: Roles of acyl-coenzyme A: cholesterol acyltransferase-1 and -2. *Curr Opin Lipidol*, 2001; 12: 289–96
6. Huang W, Li Z, Zhao L et al: Simvastatin ameliorate memory deficits and inflammation in clinical and mouse model of Alzheimer's disease via modulating the expression of miR-106b. *Biomed Pharmacother*, 2017; 92: 46–57
7. Yamamoto N, Fujii Y, Kasahara R et al: Simvastatin and atorvastatin facilitates amyloid beta-protein degradation in extracellular spaces by increasing neprilysin secretion from astrocytes through activation of MAPK/Erk1/2 pathways. *Glia*, 2016; 64: 952–62
8. Shibuya Y, Chang CC, Chang TY: ACAT1/SOAT1 as a therapeutic target for Alzheimer's disease. *Future Med Chem*, 2015; 7: 2451–67
9. Bryleva EY, Rogers MA, Chang CC et al: ACAT1 gene ablation increases 24(S)-hydroxycholesterol content in the brain and ameliorates amyloid pathology in mice with AD. *Proc Natl Acad Sci USA*, 2010; 107: 3081–86
10. Hutter-Paier B, Huttunen HJ, Puglielli L et al: The ACAT inhibitor CP-113,818 markedly reduces amyloid pathology in a mouse model of Alzheimer's disease. *Neuron*, 2004; 44: 227–38
11. Shibuya Y, Chang CC, Huang LH et al: Inhibiting ACAT1/SOAT1 in microglia stimulates autophagy-mediated lysosomal proteolysis and increases Abeta1–42 clearance. *J Neurosci*, 2014; 34: 14484–501
12. Shibuya Y, Niu Z, Bryleva EY et al: Acyl-coenzyme A: Cholesterol acyltransferase 1 blockade enhances autophagy in the neurons of triple transgenic Alzheimer's disease mouse and reduces human P301L-tau content at the presymptomatic stage. *Neurobiol Aging*, 2015; 36: 2248–59
13. Xu J, Cai R, Lu L et al: Genetic regulatory network analysis reveals that low density lipoprotein receptor-related protein 11 is involved in stress responses in mice. *Psychiatry Res*, 2014; 220: 1131–37
14. Shen Q, Wang X, Chen Y et al: Expression QTL and regulatory network analysis of microtubule-associated protein tau gene. *Parkinsonism Relat Disord*, 2009; 15: 525–31
15. Sil S, Ghosh T: Role of cox-2 mediated neuroinflammation on the neurodegeneration and cognitive impairments in colchicine induced rat model of Alzheimer's Disease. *J Neuroimmunol*, 2016; 291: 115–24
16. Shi S, Liang D, Chen Y et al: Gx-50 reduces beta-amyloid-induced TNF-alpha, IL-1beta, NO, and PGE2 expression and inhibits NF-kappaB signaling in a mouse model of Alzheimer's disease. *Eur J Immunol*, 2016; 46: 665–76
17. Liu X, Xu K, Yan M et al: Protective effects of galantamine against Abeta-induced PC12 cell apoptosis by preventing mitochondrial dysfunction and endoplasmic reticulum stress. *Neurochem Int*, 2010; 57: 588–99
18. Lu H, Li L, Watson ER et al: Complex interactions of Tyrp1 in the eye. *Mol Vis*, 2011; 17: 2455–68
19. Franco R, Martinez-Pinilla E, Navarro G et al: Potential of GPCRs to modulate MAPK and mTOR pathways in Alzheimer's disease. *Prog Neurobiol*, 2017; 149–50: 21–38
20. Giraldo E, Lloret A, Fuchsberger T et al: Abeta and tau toxicities in Alzheimer's are linked via oxidative stress-induced p38 activation: Protective role of vitamin E. *Redox Biol*, 2014; 2: 873–77
21. Tomoda H, Omura S: Potential therapeutics for obesity and atherosclerosis: Inhibitors of neutral lipid metabolism from microorganisms. *Pharmacol Ther*, 2007; 115: 375–89
22. Ding L, Biswas S, Morton RE et al: Akt3 deficiency in macrophages promotes foam cell formation and atherosclerosis in mice. *Cell Metab*, 2012; 15: 861–72
23. Yang W, Bai Y, Xiong Y et al: Potentiating the antitumour response of CD8(+) T cells by modulating cholesterol metabolism. *Nature*, 2016; 531: 651–55
24. ADAPT-FS Research Group: Follow-up evaluation of cognitive function in the randomized Alzheimer's disease anti-inflammatory prevention trial and its follow-up study. *Alzheimers Dement*, 2015; 11: 216–25
25. Yermakova AV, Rollins J, Callahan LM et al: Cyclooxygenase-1 in human Alzheimer and control brain: Quantitative analysis of expression by microglia and CA3 hippocampal neurons. *J Neuropathol Exp Neurol*, 1999; 58: 1135–46
26. Choi SH, Bosetti F: Cyclooxygenase-1 null mice show reduced neuroinflammation in response to beta-amyloid. *Aging (Albany, NY)*, 2009; 1: 234–44
27. Choi SH, Aid S, Bosetti F: The distinct roles of cyclooxygenase-1 and -2 in neuroinflammation: implications for translational research. *Trends Pharmacol Sci*, 2009; 30: 174–81
28. Dargahi L, Nasiraei-Moghadam S, Abdi A et al: Cyclooxygenase (COX)-1 activity precedes the COX-2 induction in Abeta-induced neuroinflammation. *J Mol Neurosci*, 2011; 45: 10–21

Unlike statins, genetic ablation or pharmacological inhibition of ACAT1 did not affect total cholesterol, but may decrease the level of A β in animal models [8].

Conclusions

It may be more important to explore the role of ACAT1 inhibitors in the prevention and treatment of AD. In the present study, we used siRNA interference to specifically inhibit the expression of ACAT1, and found that, compared with the A β stimulation group, pre-reduction of ACAT1 attenuated the cytotoxicity induced by A β , suggesting that ACAT1 may prove to be a meaningful target for the prevention and treatment of AD. Of course, more detailed verification is needed from animal studies.

Conflict of interests

None.

29. Choi SH, Aid S, Caracciolo L et al: Cyclooxygenase-1 inhibition reduces amyloid pathology and improves memory deficits in a mouse model of Alzheimer's disease. *J Neurochem*, 2013; 124: 59–68
30. Zhang L, Xing D, Zhu D et al: Low-power laser irradiation inhibiting Abeta25–35-induced PC12 cell apoptosis via PKC activation. *Cell Physiol Biochem*, 2008; 22: 215–22
31. Qian W, Li H, Pan N et al: Curcumin treatment is associated with increased expression of the N-methyl-D-aspartate receptor (NMDAR) subunit, NR2A, in a rat PC12 cell line model of Alzheimer's disease treated with the acetyl amyloid-beta peptide, Abeta(25–35). *Med Sci Monit*, 2018; 24: 2693–99
32. Liu T, Jin H, Sun QR et al: Neuroprotective effects of emodin in rat cortical neurons against beta-amyloid-induced neurotoxicity. *Brain Res*, 2010; 1347: 149–60
33. Millucci L, Ghezzi L, Bernardini G et al: Conformations and biological activities of amyloid beta peptide 25–35. *Curr Protein Pept Sci*, 2010; 11: 54–67
34. Fujino H, Xu W, Regan JW: Prostaglandin E2 induced functional expression of early growth response factor-1 by EP4, but not EP2, prostanoid receptors via the phosphatidylinositol 3-kinase and extracellular signal-regulated kinases. *J Biol Chem*, 2003; 278: 12151–56
35. Majumder M, Dunn L, Liu L et al: COX-2 induces oncogenic micro RNA miR655 in human breast cancer. *Sci Rep*, 2018; 8: 327
36. Pozzi A, Yan X, Macias-Perez I et al: Colon carcinoma cell growth is associated with prostaglandin E2/EP4 receptor-evoked ERK activation. *J Biol Chem*, 2004; 279: 29797–804
37. Zhi WH, Zeng YY, Lu ZH et al: Simvastatin exerts anti-amnesic effect in Abeta25–35-injected mice. *CNS Neurosci Ther*, 2014; 20: 218–26
38. McGuinness B, Passmore P: Can statins prevent or help treat Alzheimer's disease? *J Alzheimers Dis*, 2010; 20: 925–33
39. McGuinness B, Craig D, Bullock R et al: Statins for the prevention of dementia. *Cochrane Database Syst Rev*, 2016; (1): CD003160
40. Zissimopoulos JM, Barthold D, Brinton RD et al: Sex and race differences in the association between statin use and the incidence of Alzheimer disease. *JAMA Neurol*, 2017; 74: 225–32